nature geoscience

SUPPLEMENTARY INFORMATION

DOI: 10.1038/NGEO1480

Geologic methane seeps along boundaries of arctic permafrost thaw and melting glaciers

Katey M. Walter Anthony*, Peter Anthony, Guido Grosse, Jeffrey Chanton

*Correspondence and requests for materials should be addressed to K.M.W.A.

I. Supplementary Figures

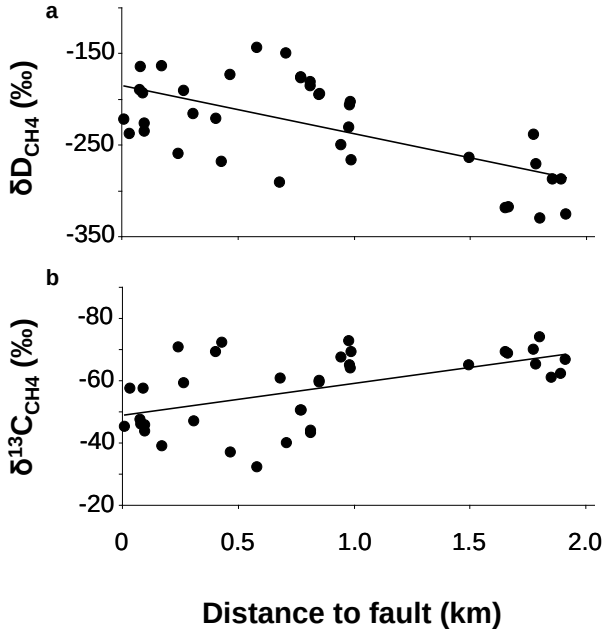

Supplementary Figure 1. The relationship between Alaska subcap seep stable isotope values and distance to faults. The δD_{CH4} (a, $p<0.001$) and $\delta^{13}C_{CH4}$ (b, $p<0.001$) values of subcap seep gases were significantly related to the distance of the seeps to mapped faults in Alaska. The relatively large spread in the data is due to the variety of precursor environmental water δD signatures and origins that subcap seeps have: deep fossil biogenic coal bed methane, thermogenic coal bed methane, thermogenic petroliferous methane, and non-fossil ^{14}C-depleted microbial methane.

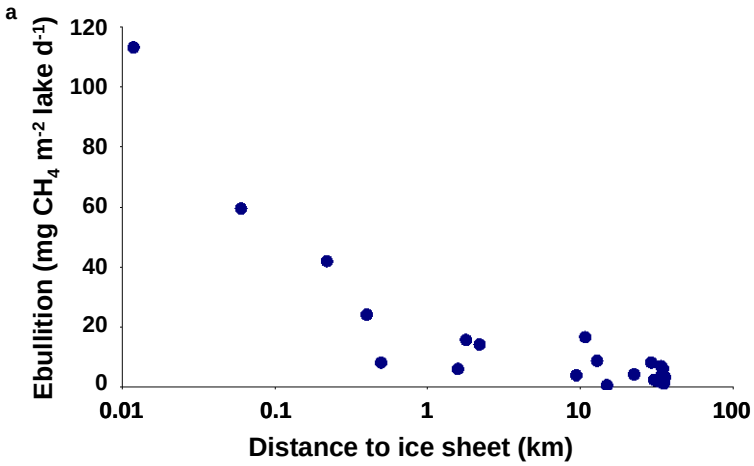

Supplementary Figure 2. Methane ebullition in West Greenland lakes. Ebullition in 25 lakes surveyed on foot decreased with distance from the ice sheet ($p<0.001$) (a). Ebullition seeps strong enough (35-847 L $seep^{-1}$ d^{-1}) to maintain large (up to 4 m^2) open holes in lake ice were found only in lakes immediately abutting the Greenland Ice Sheet, in the 1-2 km zone where glaciers have retreated during the past 100 years[38] (b). The 1-m stick shown for scale in the foreground of *b* is supported by a thin crust of white snow; ebullition had maintained a 1.5 m diameter hole free of the 0.4 m thick ice present on this lake.

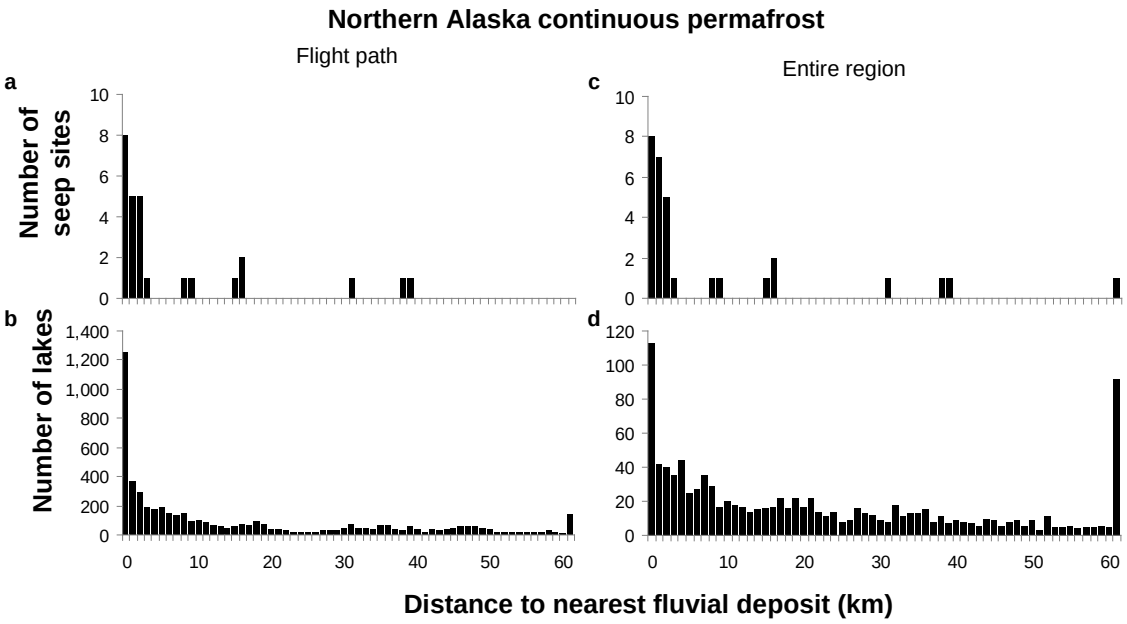

Supplementary Figure 3. Spatial relationship of subcap seeps to fluvial deposits in the continuous permafrost region of Northern Alaska. Subcap seep sites were disproportionately close to fluvial deposits in the Northern Alaska continuous permafrost region, when 27 seeps sites along the flight path (a) were compared to all 5236 lakes along the flight path (b) ($p<0.001$, One-sided, two-sample Kolmogorov-Smirnov Test) and when all 30 known seep sites across the Northern Alaska continuous permafrost region (c) were compared to a random selection of 992 lakes in this region (d) ($p<0.001$, One-sided, two-sample Kolmogorov-Smirnov Test). In the Southcentral Alaska and Interior Alaska regions, seep sites were also associated with fluvial deposits; however, the relationship was strongest in the Northern Alaska continuous permafrost region (Supplementary Table 2).

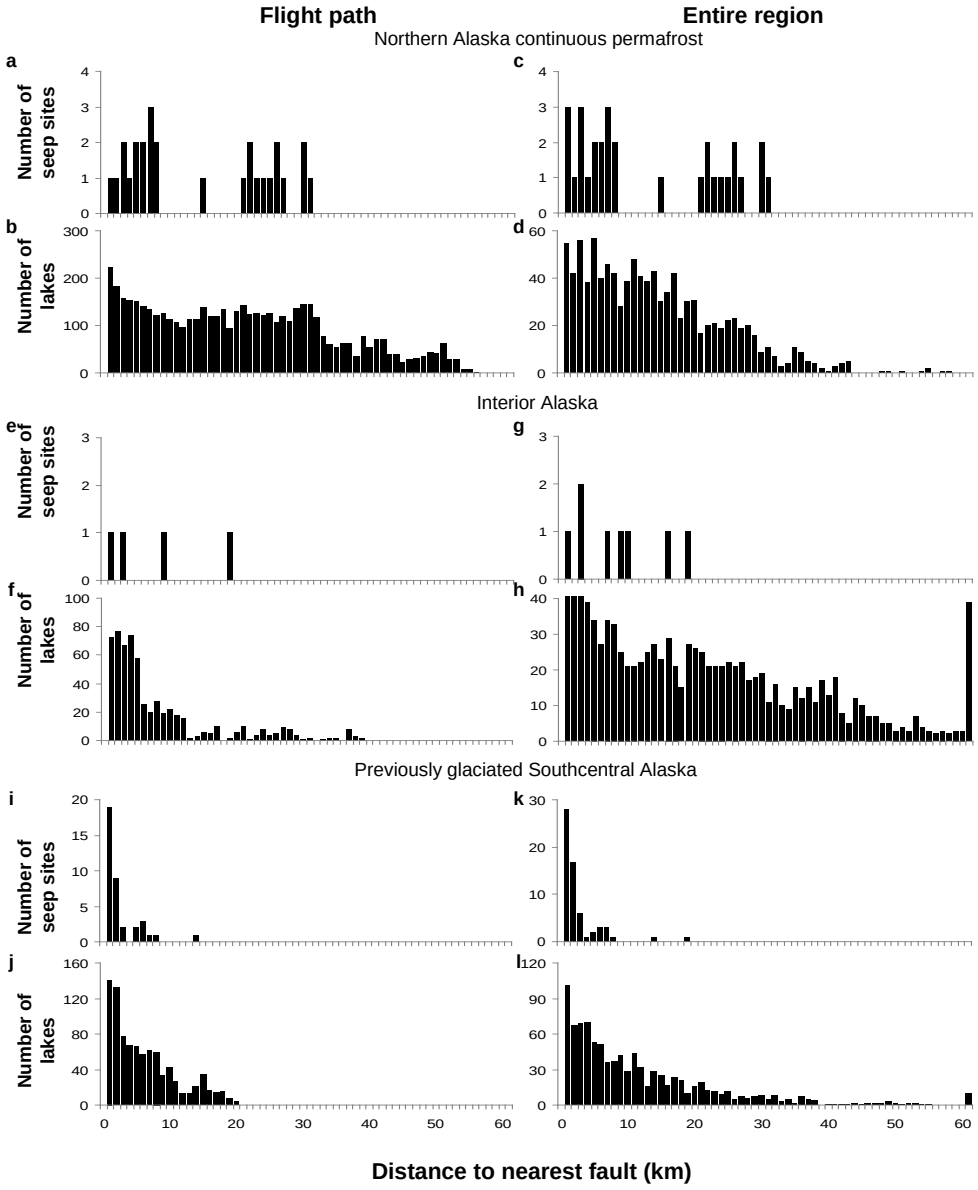

Supplementary Figure 4. Subcap seep association with mapped faults in the previously glaciated Southcentral Alaska region and lack of association in other regions. In previously glaciated Southcentral Alaska, 38 seep sites identified along the flight path were disproportionately closer to faults than all lakes along the flight path (i vs. j; $p<0.001$, One-sided, two-sample Kolmogorov-Smirnov Test). Similarly, 63 seep sites in the entire Southcentral Alaska region were disproportionately closer to faults than a random selection of 1000 lakes in

this region (k vs. l; $p<0.001$, One-sided, two-sample Kolmogorov-Smirnov Test). The number of seep sites in Interior Alaska was insufficient for statistical tests (e, f, g, h). There was no significant relationship between seep sites and faults in the Northern Alaska continuous permafrost region along the flight path (a vs. b) or in comparison to a random selection of 1000 lakes within the region (c vs. d). Results should be interpreted with a cautionary note in mind. Many of the best available databases for Alaska faults do not distinguish active from inactive faults, and many faults and surface ruptures remain altogether unmapped. Furthermore, 21 of the 63 seeps in our Southcentral Alaska study region occurred between Katalla and Icy Bay, a region with a particularly high density of active faults (Fig. 6). To ensure that our results were not an artifact of sampling sites, we compared seep sites on the survey flight path to all lakes on the flight path, and all seeps in Southcentral Alaska to 1000 randomly selected lakes in the region. In both comparisons, seeps were disproportionately associated with faults near glacier margins (Supplementary Fig. 5). Separately, removing the 21 seep sites between Katalla and Icy Bay from the analysis did not change the results: subcap seep were disproportionately associated with faults near wasting glaciers.

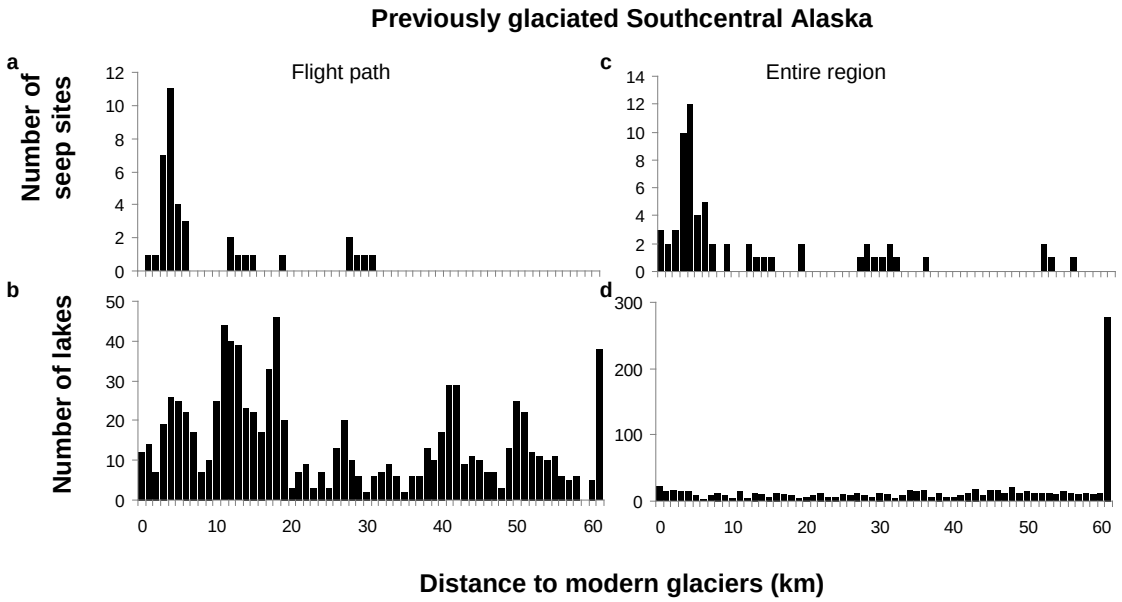

Supplementary Figure 5. The spatial relationship of subcap seeps to the extent of modern glaciers in Southcentral Alaska. Subcap seeps had a very strong association with the extent of modern glaciers in the Southcentral Alaska study region. Seep sites were nearer to glaciers than all lakes on the flight path in this region (a vs. b) ($p<0.001$, One-sided, two-sample Kolmogorov-Smirnov Test); 71% of the 38 seep sites on the flight path were within 7 km of modern glaciers as opposed to only 16% of all 902 lakes surveyed in this region. Similarly, within the entire Southcentral Alaska region that was glaciated at the Last Glacial Maximum, subcap seep sites were disproportionately closer to modern glaciers than a random selection of 954 lakes ($p<0.001$, One-sided, two-sample Kolmogorov-Smirnov test). Sixty-five percent of 63 identified subcap seep sites were within 7 km of modern glaciers, while only 11% of randomly selected lakes in the region occurred within the same proximity. These results suggest that seepage duration is finite (see Supplementary Information II.5 H4 and IV.4); therefore seeps should be less common with increasing distance from modern glaciers.

II. Supplementary Methods

II.1 *Estimating subcap seep emissions in Alaska*

The dates of aerial survey and ground truth expeditions for field work in this study are provided in Supplementary Table 4.

Following the up-scaling method of (40), to estimate subcap macroseep emissions for each site *E*, we multiplied the mean flux from subcap macroseeps measured at each site F_{avg} by the number of macroseeps *n* counted as bubble streams that caused open holes in ice at each site:

$$E = nF_{avg} \quad (1)$$

For sites where we counted open holes but did not measure flux, we assumed that mean fluxes measured at nearby sites represented fluxes in seep-induced open holes at these sites.

We suspect that our estimate of subcap macroseep emissions in Alaska is conservative for these reasons: (1) During ground truth we counted and mapped with GPS the number of open water holes and the number of individual bubble streams within holes. In all cases, our aerial survey counts underestimated the number of open holes observed in winter ground truth surveys. (2) Returning to several sites in summer, we counted the number of bubble streams in a 0.04 km^2 slough near Katalla (southern Alaska) and two lakes (area of 1.8 km^2 surveyed with boat transects) in the Brooks Range and found that we had missed 10^3-10^4 of the smaller ebullition seeps at these sites during the winter over flight. Likely the snow and ice conditions were such that these ebullition 'miniseeps' with lower bubbling rates were not observable during the time of the winter survey. Isotope values of the miniseeps were consistent with those of the larger macroseeps at these sites. This suggests that at subcap seep sites identified in aerial surveys,

numerous additional miniseeps may also exist. Miniseep emissions are estimated to be 3-4 times larger than macroseep emissions where they have been investigated outside the Arctic[26], so we suspect that excluding them from our analysis leads to an underestimation of subcap seep emissions. Supplementary Information II.6 provides an estimate of potential miniseep emissions at subcap seep sites in Alaska. (3) Our estimate of subcap seep emissions does not include potential seeps located outside water bodies such as wetlands, boreal forest, and tundra. Our method of seep detection was biased toward seeps occurring in water bodies, identified as bubbling-induced ice-free holes. While this method prohibited assessment of potential seeps in other terrestrial environments, we argue that in the northern continuous permafrost zone, seeps are more likely to occur in water bodies. Formation of open taliks (thaw bulbs) or taliks intersecting faults beneath water bodies (Fig. 4d) likely provides a conduit for gas escape through otherwise low-permeable permafrost. Nonetheless, scenarios of gas seepage through other terrestrial land surfaces are also conceivable, particularly if relict isolated taliks enclosed in permafrost or unfrozen brine pockets (cryopegs), as found in saline permafrost sediments of marine origin on the Alaska coastal plain[50], occur in the subsurface. Open shear cracks, formed by ice sheet advances, have been reported to occur in permafrost in front of ice sheets[51], and are also permeable conduits to fluid flow.

II.2 *Quantifying superficial (ecosystem) seep emissions*

We estimated methane emissions from superficial seeps following the ground survey method of (20). We removed snow from early winter lake ice to expose methane bubble clusters trapped in ice for seep classification, GPS mapping, flux measurements and gas collection. On foot, we surveyed 16,364 individual seeps within 242 snow-free plots (30-639 m^2 per plot)

placed using stratified randomization on 75 lakes to quantify superficial ebullition along the north-south transect in Alaska (Fig. 2a). Due to the high rates of superficial methane emissions from thermokarst lakes formed in yedoma-type deposits[17,19,20], we distinguished yedoma-type lakes (thermokarst lakes located in organic-rich, ice-supersaturated, silt deposits formed in unglaciated regions during the Late Pleistocene[31,52]; Fig. 2a) from non-yedoma-type lakes (occurring in all other non-yedoma deposits in permafrost and non-permafrost regions). Survey plots placed within lakes using stratified randomization revealed similar within-lake patterns of ebullition in lakes by region. However, large differences in superficial ebullition observed among regions was likely due to regional-scale differences in ecological controls over methanogenesis such as organic matter availability and climate. Following the up-scaling recommendations of (53) and pooling results of a large number of on-ice survey plots spanning a wide geographic distribution within regions, we applied mean methane ebullition measured on 26 yedoma-type lakes in Alaska (143 ± 16 mg CH_4 m^{-2} d^{-1}, n = 90 plots) to the total area of yedoma-type lakes along the north-south Alaska transect. This approach follows the EEA guidelines[45] for estimating atmospheric emissions from natural ecosystems, whereby flux measurements made at representative sources are extrapolated to all similar processes. Similarly, region-specific values measured on widely distributed non-yedoma-type lakes were applied to lakes along the transect located by region on the North Slope coastal plain (2.6 ± 1.1 mg CH_4 m^{-2} d^{-1}, n=24 plots on 15 lakes), the northern foothills of the Brooks Range (21 ± 3 mg CH_4 m^{-2} d^{-1}, n=66 plots on 14 lakes), Brooks Range and the continuous permafrost zone south of the Brooks Range (51 ± 9 mg CH_4 m^{-2} d^{-1}, n=19 plots on 5 lakes), and all other non-yedoma-type lakes south of the continuous permafrost zone (11 ± 3 mg CH_4 m^{-2} d^{-1}, n= 43 plots on 15 lakes).

II.3 *Seep flux and geochemistry*

We measured ebullition flux on 72 subcap seeps by making manual readings of gas volume trapped over 20 minutes to 2 days per seep (after 17), or for some seeps, using automated bubble traps equipped with data loggers (after 20) to measure ebullition continuously for up to 47 days. Fluxes from 106 superficial seeps were measured over periods of 2 hours to 700 days using the same methods. The long-term superficial (ecological) seep data were presented in detail in a methods paper by (20).

Gases were collected from submerged bubble traps into 60-ml glass serum vials, sealed with butyl rubber stoppers, and stored under refrigeration in the dark until analysis in the laboratory. We measured mixing ratios of C_1-C_5 alkanes and alkenes, CO_2, CO, N_2, O_2 using a Shimadzu 2014 equipped with an FID, TCD and SFID at the Water and Environmental Research Center at University of Alaska Fairbanks (UAF). A selection of replicate samples analyzed at Florida State University and the University of California, Santa Barbara confirmed results from the UAF lab. We determined $\delta^{13}C_{CH4}$ and $\delta^{13}C_{CO2}$, using a Finnegan Mat Delta V, and δD_{CH4} on a Delta XP at Florida State University. Subsamples of gas were combusted to CO_2, purified, and catalytically reduced to graphite[54], and the $^{14}C/^{12}C$ isotopic ratios were measured by accelerator mass spectrometry at the Woods Hole Oceanographic Institution's National Ocean Sciences AMS Facility, after confirmation of results by parallel analyses at the Keck Carbon Cycle AMS Facility at the University of California, Irvine. Superficial seep gases were collected and analyzed by the same methods. A subset of superficial (ecological) seep data were described by (55).

Stable isotope compositions are expressed in δ (‰) = 10^3 (($R_{sample}/R_{standard}$)-1), where R is $^{13}C/^{12}C$ or D/H and standards refer to the Vienna Pee Dee Belemnite (VPDB) and Vienna

Standard Mean Ocean Water (VSMOW), respectively. The analytical errors of the stable isotopic analyses are ± 0.1 ‰ $\delta^{13}C$ and ± 1.0 ‰ δD. We express radiocarbon data as percent modern carbon pmC (%) = $(({}^{14}C/{}^{12}C)_{sample}/({}^{14}C/{}^{12}C)_{standard}) \times 100$, which is the percentage of ${}^{14}C/{}^{12}C$ ratio normalized to $\delta^{13}C$ = -25‰ and decay corrected relative to that of an oxalic standard in 1950[54].

II.4 *Compilation of existing data from the literature*

In addition to the subcap seeps discovered in this study, we compiled for our analyses and for construction of Figure 2 records of confirmed geologic gas seeps at 24 sites in Alaska, published largely in U.S. State and Federal agency reports and maps dots[34,56-65]. Among these reports, 19 additional gas seep sites associated with mud volcanism and geothermal springs were identified (Fig. 2b), but omitted from our analysis due to their potential irrelevance to cryosphere processes. Not all mud volcanoes were reported to emit methane.

The distribution of mapped coal deposits and discovered petroleum[66-68] overlying the three cryosphere-defined regions in the geospatial analysis: Northern Alaska continuous permafrost(Fig. 2b blue shading); Interior Alaska with discontinuous, sporadic and no permafrost (Fig. 2b green shading); and the region of Southcentral Alaska (Fig. 2b grey shading) influenced by glaciers during the Last Glacial Maximum[30] (Fig. 2b hatched) are shown in Figure 2. Currently unglaciated areas of the Southcentral Alaska region contain discontinuous, sporadic and no permafrost[31]. Modern glaciers in Figure 2 are shown in white[69]; proven methane hydrate fields on the North Slope are shown as blue triangles[70]. The geology, coal and petroleum geochemistry of Alaska rocks are described in considerable detail in a number of

publications[4,34,71-76]. We considered the extent of yedoma-type deposits in Alaska defined by areas containing ice-rich eolian and retransported silt with deep thermokarst lakes[31,52].

II.5 *Geospatial Analysis*

We used geospatial analysis (ESRI™ ArcGIS 9.3) to test hypotheses (H1-H4, listed below) specific to three geographic areas in Alaska (Fig 2b). Region 1 is the northern portion of the continuous permafrost zone. Relatively small patches of currently continuous permafrost south of the Brooks Range were excluded from this zone. The Southcentral Alaska region that was covered by glaciers and ice sheets during the Last Glacial Maximum comprised Region 2. Interior Alaska with discontinuous-to-isolated permafrost (Region 3) occurs between Regions 1 and 2.

H1: Sites with subcap seeps in the Northern Alaska continuous permafrost zone should be disproportionately associated with low-ground ice content and fluvial deposits.

H2: In the previously glaciated region of Southcentral Alaska, where glacial wastage continues presently, subcap seeps should be disproportionately associated with neotectonic faults.

H3: In the Interior Alaska region, where permafrost disintegration is advanced to various levels of discontinuity, geologic seeps should be relatively rare.

H4: Geologic seeps in the continuous permafrost region should be larger than seeps in the southcentral, previously glaciated region of Alaska; and, subcap seep sites in the Southcentral Alaska region should be disproportionately closer to the extent of modern glaciers than a random selection of lakes in that region.

To test our hypotheses, we acquired various digital geospatial datasets for Alaska on permafrost[31] and lake[44] distributions, modern glacier extent[69], Last Glacial Maximum glaciation extent[30], surface geology[31] based on (77), land surface elevation (60 m resolution National Elevation Dataset for Alaska)[78], known hydrocarbon reservoirs and coal beds[66-68], sedimentary basins[61], and faults[49,61,79-82]. We additionally digitized locations of known geological methane seeps from reports and historical maps[34,49,56-65]. All datasets, available as vector data format (ArcGIS shapefile) except the raster-based land surface elevation, were projected to the same projection and coordinate system (Alaska Albers NAD83) for spatial analysis in a desktop Geographical Information System (ArcGIS).

We analyzed seep locations by the ground ice class and texture of surface sediments within the continuous permafrost region, by distance to fluvial deposits and distance to faults within all three regions, and by distance to current glacier extent within the southcentral glacial region.

To test H1 that seeps do not occur evenly across all permafrost and soil texture types, but instead are disproportionately associated with permafrost characteristics of high permeability, we used the *intersect* tool to determine the spatial relationship of seep sites to particular ground ice contents and surface sediment textures in the Northern Alaska continuous permafrost zone (Supplementary Table 1). We constructed the null hypothesis $H1_{0a}$, that seeps are independent of permafrost and soil texture types, by identifying all lakes on the transect and approximately 1000 random lakes within this zone by ground ice class and surface sediment texture.

To assess the spatial association of mapped seep sites to potential talik zones under large rivers (H1), we measured distance of seeps on our aerial surveys to fluvial deposits[31] in each region, using the *near* tool (Supplementary Fig. 3, Supplementary Table 2). As our null

hypothesis $H1_{0b}$, that seeps are independent of potential talik zones, we measured the distance to fluvial deposits of all lakes on our flight path by region, and approximately 1000 random lakes in each region. For statistical analysis of the distance distribution in each region of mapped seeps vs. fluvial deposits, lakes on transects vs. fluvial deposit, and a random selection of 1000 lakes in Alaska vs. fluvial deposit, we used the two-sample Kolmogorov-Smirnov test[83,84].

To determine the potential spatial association of subcap seeps to faults (H2), we measured the distance of seep sites in each of the three regions to the nearest mapped fault using the *near* tool in ArcGIS. For the null hypothesis $H2_{0,}$ that seeps are independent of faults, we analyzed the proximity of all lakes on our flight transect to mapped faults by measuring the distance of the geometric centroid of each lake to faults using the *near* tool (Supplementary Fig. 4). We also determined the distance distribution of a random sample of approximately 1000 lakes from the nearest fault in each of the three regions. Random lake selection across was conducted on all lakes larger 1 ha[44]. We used the Kolmogorov-Smirnov test to compare seep and lake distance to faults by region, in the same manner as the distance to fluvial deposits analysis.

We did not locate a sufficient number of subcap seeps in Interior Alaska to compare distance distributions using the Kolmogorov-Smirnov test. This paucity of seeps in the Interior confirms, in part, H3. Site-specific analysis of Interior seeps did not reveal obvious cryosphere-related controls over seep incidence.

To test H4 that seeps in glaciated Southcentral Alaska region are disproportionately close to glaciers, we measured the distance of seep sites in the southcentral region to the edge of the nearest glacier using the *near* tool in ArcGIS. For the null hypothesis $H4_0$, that seeps are independent of glaciers, we determined the distance from all lakes on our flight transect to the

nearest glacier, and also the distance of a random sample of approximately 1000 lakes in the southcentral glaciated region to the nearest glacier (Supplementary Fig. 5). Again, we used the two-sample Kolmogorov-Smirnov test to compare the distance-to-glacier distribution of observed seeps with the distance-to-glacier distribution of the $H4_0$ sample.

II.6. *Scaling current methane emissions from seeps in Alaska and the pan-Arctic*

A summary of seep emissions estimates in Alaska and the pan-Arctic and their significance in a global context is provided in Supplementary Table 3.

We estimated present-day superficial methane ebullition in Alaskan lakes (0.75 ± 0.12 Tg CH_4 yr^{-1}; standard error at the 95% confidence limits) by applying the mean measured ebullition from 90 survey plots on 26 geographically distributed thermokarst lakes in yedoma-type permafrost (52 ± 6 g CH_4 m^{-2} lake yr^{-1}) and 152 survey plots on 49 lakes outside of yedoma-type permafrost (7 ± 1 g CH_4 m^{-2} lake yr^{-1}) along the north-south transect to the total extent of these lake types in Alaska, which was 8,830 km^2 and 41,660 km^2, respectively (Fig. 2). This approach follows the EEA guidelines[45] for estimating atmospheric emissions from natural ecosystems, whereby flux measurements made at representative sources are extrapolated to all similar processes. It also meets the two most important preconditions to the applicability of emission factor approaches: comparability of emission processes and limited temporal and spatial variability.

We provided a first-order estimate of subcap macroseep emissions in Alaska (0.08 ± 0.1 Tg CH_4 yr^{-1}) following the scaling guidelines for point-source emissions of (45) and example of (40). We assumed that the point-source macroseeps observed along the flight surveys in each of the Northern Alaska continuous permafrost region (3,562,800 kg CH_4 yr^{-1} for 793 km^2 of lakes

surveyed), the Interior Alaska region (6,951 kg CH_4 yr^{-1} for 38 $km^2$of lakes surveyed), and the previously glaciated Southcentral Alaska region (168,931 kg CH_4 yr^{-1} for 169 km^2 of lakes surveyed) were a representative sample of subcap seeps for all lakes in these zones across the rest of Alaska. We cross-checked this estimate using the median point-source emission values for each 50-km wide latitudinal bin, and found that the point-source subcap seep emissions would be 10% lower due to under-representation in this scaling method of some rare, but high point-source seep fields. While the mean value may be considered less robust than using a median, the mean provides a closer to actual total when multiplied by area because it adequately considers those data points with high fluxes that contribute most significantly to the total[40]. The uncertainty value for the Alaska subcap emission estimate was derived by propagating errors of the estimates of number of seeps per site and seep flux (kg CH_4 $seep^{-1}$ d^{-1}) for all measured and estimated sites in the three Alaska study regions at the 95% confidence limits.

To estimate the potential contribution of subcap miniseeps to total subcap ebullition in Alaska, we upscaled detailed measurements of subcap 'miniseeps' at three Alaska study sites. At two northern sites and one southcentral site, we measured the density of small ebullition miniseeps in different areas, their methane ebullition rates, and stable isotope values. We found miniseeps were an order of magnitude more abundant than macroseeps and had similar isotope values; however, due to lower ebullition rates, adding miniseep emissions to macroseeps increased the estimate of subcap emissions from these sites by only 3-fold. To scale up subcap emissions to the state of Alaska, we assumed that the ratio of miniseep-to-macroseep fluxes (2.0 ± 0.4, standard deviation) observed at the limited number of field sites applies to all observed macroseep sites. Our observation of 10^3-10^4 miniseeps at 100% of the eight sites in Alaska where we had the potential to see miniseeps due to summertime or snow-free conditions lends support

to this assumption. The cumulative estimate of macroseep (0.08 ± 0.01 Tg CH_4 yr^{-1}) plus miniseep (0.17 ± 0.03 Tg CH_4 yr^{-1}) subcap seepage in Alaska is 0.25 ± 0.03 Tg CH_4 yr^{-1}.

Diffuse microseepage of geologic methane has been recognized throughout large areas over oil and gas fields on various continents[25]. A large number of systematic measurements over dry lands have shown that the positive flux of methane, or microseepage, is quite common and pervasive within petroliferous and sedimentary basins in the range of 0-5 mg CH_4 m^{-2} d^{-1}, and can reach levels of 10-10^3 mg CH_4 m^{-2} d^{-1} throughout large areas, especially around mud volcanoes[85,86]. Statistical analysis of the global microseepage data set suggests that microseepage from the world's petroliferous and sedimentary basins outside the cryosphere region is 10-25 Tg CH_4 yr^{-1} (25). While we did not measure microseepage in Alaska, we conducted a theoretical analysis of the potential microseep emission, which we assumed was independent of subcap macroseeps, for all currently unfrozen soils of Alaska that have been mapped as oil, gas or coal measures[66,67] or as hydrocarbon-prone sedimentary basins[61,87], defined as portions of sedimentary basins that are, or have been in the past, at temperatures >70 °C (thermogenesis)[25]. Due to limitations in the thermal resolution of the Alaska data set[61] after (87), we conservatively considered only portions of sedimentary basins that are, or have been in the past, at temperatures >95 °C. In our calculations the potential microseepage areas had minimum and maximum potential extents based on the definition and coverage in Alaska of permafrost types by unfrozen ground fraction: continuous (~10% unfrozen), discontinuous (10-50% unfrozen), and sporadic/isolated (>90% unfrozen, we assumed 95%)[31,46]. To these potential microseepage areas we applied the microseepage fluxes statistically evaluated on a global basis in (25) to estimate current potential geologic methane microseepage in unfrozen, hydrocarbon-prone soils of Alaska: 0.5-1.1 Tg CH_4 yr^{-1}.

Following the scaling methods of (40 and 45), we estimated the potential magnitude of present day subcap macroseep emissions from pan-arctic lakes overlying assumed natural gas fields in the continuous permafrost zone north of ~60°N based on the U.S. Geological Survey's Circum-Arctic Resource Appraisal[2] and our limited macroseep flux data set from Alaska. Our first-order estimate of 0.70 ± 0.1 Tg CH_4 yr^{-1} for macroseepage subcap emissions is the product of (a) the aggregate subcap methane emissions observed along our survey flight path in the northern continuous permafrost zone (3.6 x 10^6 kg CH_4 yr^{-1}) divided by the total area of lakes surveyed in this zone of the flight path (793 km^2)] and (b) the area of large pan-arctic lakes[46] overlying assumed natural gas fields[2] (150,000 km^2). Since the pan-arctic emission estimate is based on geospatial seep relationships derived in Alaska, we calculated the error around the pan-arctic estimate based on propagation of the error for the Alaska subcap macroseep emission estimate at the 95% confidence limits. We acknowledge large uncertainties behind this estimate because Alaska's hydrology and geology differ in many respects from other regions of the pan-Arctic. However, there are universal controls on the cryosphere; similar observations of fossil methane trapped within and beneath permafrost have been documented in Russia[8,15] and Canada[3,88,89]; and thermogenic methane release through a high discharge seep field in a lake on the Mackenzie Delta, NWT, Canada has been attributed to permafrost thaw[16].

Our first order estimate of pan-arctic subcap seep emissions likely under-represents subcap seep emissions in the Arctic for the following reasons: (1) Our extrapolation was based on the area of assumed natural gas fields[2] in the continuous permafrost zone north of ~60 °N, so it neglects natural gas fields beneath permafrost that occurs south of this latitude. (2) We did not account for ^{14}C-depleted methane originating from glacial sediments associated with glaciers and ice sheets[13,90], or with the extensive occurrences of coal beds and other buried organic-rich

deposits beneath permafrost and glaciers in sedimentary basins in the pan-Arctic[91]. (3) Our flux measurements of subcap seeps were made during short-term field campaigns, and measurements made over times scales of hours to days likely captured quiescent 'background' seepage rates rather than the more prolific, but rare eruption events that have been described at other geologic seep sites[92-94]. It is likely that larger-than-observed emission events occur with subcap seeps too, based on our field observations of inactive pockmarks and pockmark sizes that were sometimes disproportionately large compared to the size of the bubble streams observed therein. (4) Our estimate does not account for potential diffusive microseep emissions, which are assumed based on (25) to occur independent of subcap macroseeps in the Arctic, and which are known to dominate geologic emissions in other terrestrial environments in Europe, Central Asia, China and the United States[25].

II.7 *Greenland seep surveys*

We quantified methane seep ebullition from 25 lakes in the region of Kangerlussuaq, Greenland (67.0° N, 50.7° W) by ground surveys only, following the method of (20) and in accordance with recommendations to survey ebullition seeps trapped in ice over large spatial scales in lakes[53]. Due to ideal conditions of 15-40 cm lake ice thickness with no snow cover in late November 2010, we were able to conduct extensive surveys by foot (up to 9,000 m^2 per lake along 1-m wide survey swaths spanning entire lakes in multiple directions). We mapped 1,135 seeps individually with GPS on the 25 lakes. In the majority of lakes we found either no bubbling or the small (primarily 0.001 to 0.1 L d^{-1}), ice-trapped bubbles typical of superficial seeps. Ebullition seep emissions increased with proximity to the ice sheet (Supplementary Fig. 2). Only in lakes directly adjacent to the ice sheet, in the 1-2 km zone where glaciers have

retreated during the past 100 years[38], did we find highly ebullient subcap seeps, with individual holes as large as 4 m^2 in ice of 40 cm thickness. Outside of this zone we found no ebullition-induced open holes in lake ice. The radiocarbon age of methane collected from three high discharge seeps in the glacial retreat zone was 1420 ± 25 yrs, 1420 ± 25 yrs, and 1530 ± 40 yrs; whereas methane collected from a representative superficial flux seep in a lake 9.5 km from the Greenland ice sheet had a modern radiocarbon age (pmC 107%). Stable isotope values ($\delta^{13}C_{CH4}$, -66.8 to -62.7‰; δD_{CH4}, -402 to -359‰) and the absence of C_2+ hydrocarbons in the gas samples suggest that methane formed microbially in the Greenland seeps. In this West Greenland site, where the major ice sheet retreat occurred prior to 6,000 cal. yr.BP[95], the ice sheet has advanced and retreated over spatial scales of 1-2 km during the past several thousand years in conjunction with the c. 2000 BP neoglacial event and Little Ice Age[38]. Various botanic, geomorphologic, and geochronological indicators suggest that the ice sheet has retreated at our study site 1-2 km over the past 100 years, coincident with peripheral thinning[38]. The radiocarbon ages of methane from seeps within this zone of glacial advance and retreat were similar to the ages of vegetation that would have established in this zone in between the c. 2000 BP neoglacial event and the Little Ice Age. Given that little or no modern vegetation was observed immediately adjacent to lakes containing the high discharge seeps, and that the highly turbid lake water with glacial silt was unlikely to support significant aquatic productivity during the current time, it is likely that the decomposition of organic matter beneath the ice sheet occurred after the Little Ice Age advance, and that with recent ice sheet retreat, the ^{14}C-depleted methane now escapes to the atmosphere. Large quantities of organic-rich sediments, including coal, petroleum-associated hydrocarbons and glacially-buried organics, are also known to occur in both the marine and

terrestrial regions of Greenland[96-98]; however, to our knowledge, none have been reported immediately at the Kangerlussuaq study site.

III. Supplementary Tables

Supplementary Table 1. The occurrence of subcap seep sites in relation to permafrost ice content and soil texture in the Northern Alaska continuous permafrost region. The Seep Ratio is the ratio of the fraction of seeps located within a specific permafrost-ice or soil texture class to the fraction of randomly selected lakes occurring in these permafrost soil classes. High seep ratios between seep sites (a) and both the number of randomly selected lakes (b) and their area (c) revealed that seeps occurred disproportionately in the low and variable ice classes, and in the coarsest sediment texture class (rocky). These findings support H1, in that seeps did not occur evenly across all permafrost types, but were disproportionately located in permafrost types indicative of higher permeability for gas flow (e.g. low ground ice content and coarse, fluvial sediments). It is possible that gas migration through fractured bedrock, faults or fractures intersected by extant or relict thaw bulbs, unfrozen saline horizons, or fine-grained sediments with a high unfrozen water content[99-102] could account for the occurrences of rarer seeps located in lakes situated in other permafrost soil types.

		A		**B**			**C**		
		Number of Seeps	Percent	Number of lakes	Percent	Seep ratio	Lake area (km^2)	Percent	Seep ratio
Permafrost ice content	Low	16	55%	33,014	31%	1.8	4,547	35%	1.6
	Moderate	5	17%	45,113	42%	0.4	5,617	43%	0.4
	Variable	5	17%	9,314	9%	2.0	702	5%	3.2
	High	3	10%	19,523	18%	0.6	2,259	17%	0.6
Texture	Rocky	10	34%	17,328	16%	2.1	1,188	9%	3.8
	Sandy	16	55%	63,004	59%	0.9	8,892	68%	0.8
	Silty	3	10%	26,632	25%	0.4	3,044	23%	0.4

Supplementary Table 2. Comparison of seep association with fluvial deposits among the three Alaska study regions: Northern Alaska continuous permafrost, Interior Alaska, and the previously glaciated Southcentral Alaska region. Percentages reflect the fraction of subcap seep sites or the fraction of 1000 randomly selected lakes that occurred within 3 km of mapped fluvial deposits, a distance that takes into account the mapping inaccuracy for fluvial deposits. Within each of the regions, percentages of seep sites within 3 km of fluvial deposits were greater than the percentages of a random selection of lakes in the regions. The relationship between subcap seeps and fluvial deposits was strongest in the Northern Alaska continuous permafrost region.

Region	1000 lakes	Seep sites
Northern Alaska continuous permafrost	22%	70%
Interior Alaska	41%	50%
Southcentral Alaska previously glaciated	23%	51%

Supplementary Table 3. Summary of current and future global seep emissions.

Current global emissions	Tg CH_4 yr^{-1}	Implications
Alaska		
Subcap macroseeps	0.08 ± 0.01	Primary measurement in this study. Comparable to the scale of natural geologic emissions from other terrestrial regions of the globe, except that in Alaska emissions are concentrated along boundaries of cryosphere retreat.
Subcap miniseeps	0.17 ± 0.03	Extrapolating measured miniseep emissions from a subset of study sites to all subcap sites increases the estimate of subcap emissions in Alaska ~3-fold.
Total subcap seeps	0.25 ± 0.03	The sum of subcap macroseeps plus miniseeps.
Geologic microseepage	0.5 - 1.1	Not measured, but theoretically determined for unfrozen hydrocarbon-prone sedimentary basin soils in Alaska following (25). Geologic microseepage, assumed to be independent of subcap seeps, is 2-5 times larger than emissions from the later.
Total geologic seepage	0.7-1.4	Total emissions from geologic microseepage, subcap macroseeps, and subcap miniseeps is comparable in magnitude to superficial, ecosystem emissions from Alaskan lakes.
Superficial seeps	0.75 ± 0.12	At present superficial seeps from ubiquitous ecological sources in Alaska's lakes cumulatively emit about three times more methane than locally constrained subcap macroseeps and miniseeps.
Geologic + subcap + superficial seepage	1.5 - 2	Together geologic microseepage, subcap seeps, and superficial ebullition seeps in Alaska's lakes increase the current estimate of natural methane emissions in Alaska[39] by 50-70%.
Alaska wetland ecosystems	3	Net ecosystem emissions from Alaska wetlands, from (39). Emissions from lakes not included.
Pan-arctic continuous permafrost		
Subcap macroseeps	0.7 ± 0.1	Extrapolation of geospatial relationships of subcap macroseeps in the Northern Alaska continuous permafrost zone to the region of assumed natural gas fields[2] in the terrestrial pan-arctic continuous permafrost zone north of 60° N.
Subcap miniseeps	1.4 ± 0.25	Assumes the same proportional relationship between macroseeps and miniseeps in the pan-Arctic as was observed in Alaska.
Subcap macroseeps + miniseeps	2 ± 0.3	Increases the estimate of global macroseepage from terrestrial regions[26] by >50%. Not included are subcap seeps associated with permafrost thaw south of 60°N or with pan-arctic areas of glacial and ice sheet wastage.
Global		
Geologic macroseeps + miniseeps	3-4	From (26)
Geologic microseepage	10-25	From (25)
Future seepage		
Subcap seepage		A large, but transient expulsion of subcap methane is expected to increase surface carbon cycling with implications for greenhouse gas feedbacks to climate warming in a future scenario of widespread permafrost thaw and wastage of glaciers and ice sheets. The magnitude and timing of this emission scenario is unconstrained due to large uncertainties in estimating future rates of cryosphere degradation, hydrocarbon reservoir response, and potential methane oxidation.
Long term microseepage (Alaska)	~2.5	This scenario applies to a far-distant future when permafrost has become sufficiently degraded and subcap methane has already largely escaped. We expect geologic microseepage to occur in unfrozen hydrocarbon-prone sedimentary basins in proportion to its global rates[25], controlled by geologic and biogeochemical processes. Future microseepage rates in Alaska could be 2-5 times higher than at present.
Long term microseepage (pan-Arctic)	~11	Applying global microseepage rates based on (25) to the area of assumed natural gas fields[2] in the pan-Arctic north of 60° N in the far-distant future scenario, would produce new microseepage emissions from a region that is today capped by continuous permafrost. Future microseepage from this region would increase global microseepage emissions by ~40-100%.

Supplementary Table 4. Dates of aerial surveys and ground truth field campaigns for subcap seeps.

Region	Aerial Survey	Field work
North Slope Alaska		July 2007
		January 2008
		April 2008
	October 2008	October 2008
		May 2009
	October 2009	October 2009
		March 2010
		July 2010
Brooks Range Alaska	October 2009	-
	February 2010	February 2010
		September 2010
		April 2011
Interior Alaska	October 2009	-
	February 2010	February 2010
		April 2010
	October 2010	October 2010
	November 2010	November 2010
		April 2011
Southcentral Alaska	February 2009	February 2009
		August 2009
	January 2010	January 2010
	February 2010	February 2010
		April 2010
		May 2010
		June 2010
Kangerlussuaq, Greenland		November 2010

IV. Supplementary Discussion

IV.1 *Subcap seeps association with fluvial deposits*

Geospatial analysis revealed that subcap seeps had a disproportionately high proximity to fluvial deposits in the Northern Alaska continuous permafrost region (H1). Along the north-south flight path, we found that 70% of seep sites as opposed to only 40% of surveyed lakes occurred within 3 km of mapped fluvial deposits in the northern permafrost zone[31] (Supplementary Fig. 3). We used a 3 km buffer in order to address local inaccuracies in the mapping of fluvial deposits[31]. Similarly, a comparison of all documented subcap seep sites in the northern continuous permafrost zone of Alaska with a random selection of lakes in this region revealed that 70% of seep sites and only 22% of surveyed lakes occurred within 3 km of mapped fluvial deposits of larger rivers. This relationship of subcap seeps to fluvial deposits was stronger for the continuous permafrost zone than all other regions of Alaska (Supplementary Table 2), and supports our hypothesis that seeps occur in areas of permafrost with steep thaw gradients (H1) for several reasons. First, fluvial deposits, which occur as thick accumulations of unconsolidated sediments[4,103], are more permeable for fluid flow than bedrock, dense silt or clay[3,104]. Furthermore, fluvial sediments are deposited as a result of flowing water, a process that efficiently transfers heat into the subsurface, facilitating rapid thaw of permafrost and opening of conduits, such as through taliks, for gas migration through the cryosphere cap. Several outlier seeps up to 39 km from fluvial deposits could potentially be explained by unmapped smaller fluvial deposits, buried fluvial deposits, ice poor and coarse-textured sediments or bedrock, or by active faults in the Brooks Range, a region with few remaining glaciers today, but which was also glaciated at the Last Glacial Maximum[30]. It is also possible for gas to migrate through ice-

poor permafrost in fractured bedrock or coarse textured sediments without being capped[3,15].

IV.2 *Subcap seeps association with faults adjacent to melting glaciers*

Subcap seeps had a high association with faults and proximity to modern glaciers in Southcentral Alaska, the study region that was covered by glaciers during the Last Glacial Maximum glaciation[30,31] (Supplementary Figs. 4 and 5). We did not find a statistically significant relationship between seep sites and faults in the Northern Alaska continuous permafrost zone or Interior Alaska. In the previously glaciated southcentral region of Alaska, we found that sites with subcap seeps along the aerial survey flight path were more likely to occur in close proximity to mapped faults than all lakes on the flight path (H2); 79% of seep sites and 39% of all lakes along the southern portion of the flight path were located within 3 km of the nearest mapped fault. This relationship was consistent when we compared the association of all documented seeps in the previously glaciated region of Southcentral Alaska with a random selection of lakes in this zone. Within the entire previously glaciated zone, 81% of seep sites were located within 3 km of the nearest fault, while only 25% of 954 randomly selected lakes within this zone were within 3 km of the nearest fault. The exceptionally high correlation between seep sites and faults for the Katalla region on the Gulf of Alaska (Fig. 6e), where 90% of seep sites fell within 1 km of mapped faults using recently available high resolution neotectonic faults information[49] (T. Pavlis, personal communication, May 14, 2010), suggests that the strength of the association between faults and seeps is limited by the resolution of fault mapping available in Alaska, and that ebullition seeps could be useful indicators of active faults to aid future mapping. The same strong relationship between seeps and active faults was observed 170 km to the southeast by the Bureau of Land Management's earlier hydrocarbon

exploration, the records from which indicate that "in Icy Bay, Yakataga, ...gas seeps are found on almost all of the streams draining the [Sullivan] anticline southward into the sea. Most of the seeps are found along a narrow belt along the fault plane of the anticline[64]."

The relative proximity of seep sites observed in this study to the boundary of modern glaciers in Alaska (Supplementary Fig. 5) suggests a potential relationship to changes in the glacial cryosphere. Modeling studies suggest that deglaciation perturbs the hydrodynamic conditions of hydrocarbon systems in sedimentary basins[11,13,14]. Cryosphere disintegration may lead to isostatic uplift, and such uplift may release formerly dissolved gas from sediment pore water in hydrocarbon reservoirs, leading to new accumulations of natural gas[14], and its potential escape to the atmosphere through permeable strata. During periods of glacial expansion, fluid migration pathways may also form in the subsurface when differential ice loading fractures sediment units through flexure or overpressure; however, gas remains trapped in or beneath the impermeable seal of ice or methane hydrates during glacial periods, and is released to the atmosphere during deglaciation[11]. Finally, there is the indirect effect of isostatic rebound-related seismicity on gas seepage. Ice melt on glaciers reduces the normal stress on the ground caused by the overburden of massive ice. Reduction in normal stress enhances fault activity and opening of joints. These seismic responses associated with isostatic rebound are known to occur in our Southcentral Alaska study region[32,33,35], and are a likely mechanism for the increase in subcap methane seepage associated with glacial wastage in this region.

The close distance relationship of seeps to glaciers also implies that the duration of subcap gas seepage associated with glacial wastage is limited to time scales of centuries to several millennia as glaciers pull back and thin (H4, Supplementary Information IV.4). This 100-3,000 year time scale is also supported by model predictions of methane emissions and gas

hydrate stability zone destabilization associated with cryosphere disintegration in other regions such as Europe[14] and North America[13]. Therefore, areas unglaciated or lacking continuous permafrost for thousands of years (e.g. Interior Alaska) have fewer seeps today (H3).

IV.3 *Variability in methane radiocarbon age of subcap seeps in Alaska and Greenland*

The majority of subcap seeps in Alaska emitted ^{14}C-dead methane; however subcap seeps at two sites in regions with ongoing glacial wastage contained detectable amounts of $^{14}C_{CH4}$: the Lake Eyak region in Southcentral Alaska and the West Greenland lakes abutting the ice sheet. Two plausible explanations for the measurable ^{14}C at these sites are (1) methane was formed microbially beneath the glaciers after organic matter was buried by the glaciers; and subsequent glacier retreat has allowed for the current escape of this ^{14}C-depleted methane to the atmosphere. Several lines of evidence support this explanation: a) stable isotopes suggest microbial formation of methane in the seeps with the highest levels of ^{14}C (Fig. 6); b) the age of the methane emitted at these sites corresponds to the age of the organic matter that would likely have been buried by the last glaciation at the sites; and c) we found a strong relationship between $\delta^{13}C_{CH4}$, $^{14}C_{CH4}$ and distance to faults in the Lake Eyak site, where fault data exist (Fig. 6), suggesting that faults allow the escape of deeper, more ^{14}C-depleted methane to the atmosphere. In Greenland, where the ice cap is thought to prohibit the stress release from glacial mass loss in earthquakes[105], the subcap seeps are unlikely to have a seismic association. It is possible that they occur in relationship to newly discovered 'glacial earthquakes'[106] in Greenland, but to our knowledge, these have yet to be recorded at the Kangerlussuaq study site. (2) During ascent through the sediments, ^{14}C-dead or ^{14}C-depleted methane entrains methane formed in shallower sediments from microbial decomposition of younger organic matter, thereby diluting the ^{14}C-

depleted signal of the subcap seep gas[6,92]. The fact that seeps in the vicinity of Lake Eyak fell along a tight isotopic mixing line between two end members of ^{14}C-enriched biogenic methane and ^{14}C-dead thermogenic methane (Fig. 6) suggests that both explanations (1) and (2) could be appropriate for this site. We found a similar relationship between subcap methane stable isotopes and distance to faults across all of Alaska (Supplementary Fig. 1). Finally, although ebullition is typically thought to transport gas at a rate that exceeds microbial oxidation, we cannot rule out the possibility that some isotopically enriched methane released from subcap seeps is the result of aerobic or anaerobic methane oxidation that occurs within or beneath permafrost and glaciers over long periods of time prior to escape.

IV.4 *Magnitude and duration of subcap seepage*

When a conduit to gas escape through the cryosphere opens, the precise magnitude and duration of seepage that follows is unknown. They are likely a function of longevity of the cap[107], reservoir size, pressure, temperature, and flow rate, and are dependent on the presence and configuration of open geological conduits such as fractured bedrock, open joints, faults, fissures, or unconsolidated sediments with sufficient permeability[11]. Based on multiple lines of evidence at the Alaskan sites, we expect gas escape to occur over time scales of centuries to millennia once conduits open and remain open: (1) Seeps in areas that were glaciated during the Little Ice Age advances in Alaska and Greenland were disproportionately close to the modern glacial boundaries; (2) We observed relatively few geologic seeps in Interior Alaska where a continuous cryosphere cover has been absent since the Holocene Thermal Maximum (11,000-9,000 years BP)[113], and where cryosphere-related gas conduits may have since opened and depleted their cryosphere-capped reservoirs; (3) The strongest seeps were found on the North

Slope (Figs. 2 and 4), where permafrost is thickest along a latitudinal gradient in Alaska, suggesting the possibility for the greatest longevity of the cap[107] and the largest release upon its disintegration; (4) personal accounts and records of currently active seeps on the Alaska North Slope dating back 65 years[114] and 66 years[115].

IV.5 *Future subcap methane emissions*

While models generally predict that time scales far beyond 2100 are required for continuous permafrost to degrade into discontinuous permafrost[1,41,116,117], the scenario that would likely lead to a large, but transient expulsion of geologic methane trapped within and beneath permafrost, field observations of the thermal state of permafrost in Russia revealed that continuous permafrost has already begun to thaw in some locations and that the border between continuous permafrost and discontinuous permafrost has migrated northward during recent decades[42].

Furthermore, complete thaw of permafrost is not essential for gas migration since warming widens existing taliks and increases the unfrozen water content of permafrost, particularly for fine grain facies, allowing fluid migration along temperature gradients[99-102]. The increase in continuous permafrost permeability to gas flow could be greatly accelerated by an increase in the extent and volume of existing open taliks and formation of new taliks in response to the combined effect of climate warming, permafrost warming, and intensification of sub- and supra-permafrost water exchange[43].

Finally, our findings suggest that predictions of increased seismic activity, earthquake frequency and faulting associated with deglaciation and shrinkage of the modern ice sheets in Greenland and Antarctica[118], where extensive coal and conventional hydrocarbons are known to

occur[96-98,119-122], could also be accompanied by the release of large quantities of methane through future fault activation, serving as an additional, so-far unconstrained positive feedback to climate warming. While it is unknown how much subcap methane will reach the atmosphere or its affect on global climate due to difficulties in extrapolating future rates of cryosphere degradation, hydrocarbon reservoir response, and future potential methane oxidation rates, an increase in surface carbon cycling with implications for greenhouse gas emissions is likely.

IV.6. *Post-cryosphere geologic emissions in Alaska and the pan-Arctic*

Once cryosphere-capped methane pools have been released to the atmosphere following cryosphere degradation, deep-sourced methane emissions should be similar to those outside of the cryosphere region[8,10,24-26], governed by local geology. For example, the potential geologic microseepage emissions in a far-distant future when permafrost in Alaska and the pan-Arctic will have significantly degraded and subcap methane will have already largely escaped, we expect geologic microseepage to occur in unfrozen hydrocarbon-prone sedimentary basins in proportion to its current global rates[25], controlled by geologic and biogeochemical processes. We estimate that future microseepage rates could be 2-5 times higher in Alaska than at present, and that at the pan-arctic scale, microseepage from the assumed natural gas fields on land north of 60° N (3.5×10^6 km^2) based on (2) would be ~11 Tg CH_4 yr^{-1} (Supplementary Table 3), increasing the current global microseepage rate by 40-100%.

V. Supplementary Notes

50. Williams, J. R. *Ground water in the permafrost regions of Alaska* (US Dept Interior, USGS Professional Paper 696, 1970).
51. Scholz, H. & Baumann, M. An "open system pingo" near Kangerlussuaq (Søndre Strømfjord), West Greenland. *Geology of Greenland Survey Bulletin* **176**, 104-108 (1997).
52. Kanevskiy, M., Shur, Y., Fortier, D., Jorgenson, M. T. & Stephani, E. Cryostratigraphy of late Pleistocene syngenetic permafrost (yedoma) in northern Alaska, Itkillik River exposure. *Quat. Res*. doi:10.1016/j.yqres.2010.12.003 (2011).
53. Wik, M., Crill, P. M., Bastviken, D., Danielsson, Å., & Norbäck, E. Bubbles trapped in arctic lake ice: Potential implications for methane emissions, *J. Geophys. Res.* **116**, G03044 (2011).
54. Stuiver, M. & Polach, H. Reporting of ^{14}C data. *Radiocarbon* **19**, 355-363 (1977).
55. Walter, K. M., Chanton, J. P., Chapin III, F. S., Schuur, E. A. G. & Zimov, S. A. Methane production and bubble emissions from arctic lakes: Isotopic implications for source pathways and ages. *J. Geophys. Res*. **113**, G00A08 (2008).
56. Pavlis, T. Personal communication of terrestrial gas seeps observed near the Gulf of Alaska (2010).
57. Motyka, R. J., Moorman, M. A. & Liss, S. A. *Geothermal resources of Alaska*,1 map sheet, scale 1:2,500,000 (State of Alaska, Dept. Nat. Res., Alaska Division of Geological and Geophysical Surveys Miscellaneous Publication 8, Fairbanks, 1983).
58. Motyka, R. J., Hawkins, D. B., Poreda, R. J. & Jeffries, A. *Geochemistry, Isotopic composition, and the origin of fluids emanating from mud volcanoes in the Copper River*

Basin, Alaska (State of Alaska, Dept. Nat. Res., Alaska Division of Geological and Geophysical Surveys, Public-data File 86-34, Fairbanks,1986).

59. Motyka, R. J., Liss, S. A., Nye, C. J. & Moorman, M. A. *Geothermal Resources of the Aleutian Arc,* 4 map sheets (State of Alaska, Dept. Nat. Res., Alaska Division of Geological & Geophysical Surveys, Report of investigations 114, Fairbanks, 1993).
60. Symonds, R. B. *et al. Investigations of gas seeps and springs in the vicinity of The Gas Rocks, south shore Becharof Lake, Alaska* (US Dept Interior Rep., USGS Open-File Report OF 97-0127, 1997).
61. Troutman, S. M. & Stanley, R. G. *Maps showing sedimentary basins, surface thermal maturity, and indications of petroleum in the Central Alaska Province,* scale 1:2,500,000 (US Dept Interior, USGS Miscellaneous Field Studies Map MF-2428, 2003).
62. Reifenstuhl, R., Bailey, R. D. & Finzel, E. S. *Bristol Bay and Alaska Peninsula 2004: Fieldwork and Sample Analyses Compilation Report* (State of Alaska, Dept. Nat. Res., Alaska Division of Geological and Geophysical Surveys, PIR 2005-1, Fairbanks, 2005).
63. Blodgett, R. B. & Clautice, K. H. *Oil and gas seeps of the Puale Bay - Becharof Lake - Wide Bay region, northern Alaska Peninsula,* 1 map sheet, scale 1:250,000 (State of Alaska, Dept. Nat. Res., Alaska Division of Geological and Geophysical Surveys, Preliminary Interpretive Report 2005-6, Fairbanks, 2005).
64. Blasko, D. P. *Oil and gas seeps in Alaska: Alaska Peninsula, western Gulf of Alaska* (US Dept. Interior Rep. 8122, Bur. Mines, Washington D.C., 1976).
65. Decker, P. L. & Wartes, M. A. *Geochemistry of the Aupuk gas seep along the Coleville River – Evidence for a thermogenic origin* (State of Alaska, Dept. Nat. Res., Alaska Division of Geological and Geophysical Surveys, PIR 2008-1E, Fairbanks, 2008).

66. Ehm, A. *Oil and gas basins map of Alaska,* 1 map sheet, scale 1:2,500,000 (State of Alaska, Dept. Nat. Res., Alaska Division of Geological & Geophysical Surveys Special Report 32, Fairbanks, 1983).

67. Merritt, R. D. & Hawley, C. C. *Map of Alaska's coal resources,* 1 map sheet, scale 1:2,500,000 (State of Alaska, Dept. Nat. Res. Special Report 37, Division of Geological & Geophysical Surveys, Fairbanks, 1986).

68. Beaty, C. 2005. *Compilation of publicly known oil, gas and hydrate accumulations* (State of Alaska, Dept. Nat. Res., Div. Oil and Gas, Anchorage, 2005).

69. Information Resource Management Section. *Alaska Glaciers* 1:1,000,000 (State of Alaska, Dept. Nat. Res., Fairbanks, 1998.

70. Collett, T. S. *et al*. Permafrost associated natural gas hydrate occurrences on the Alaska North Slope. *Marine and Petroleum Geology*, doi:10.1016/j.marpetgeo.2009.12.001 (2010).

71. Carman, G. J. & Hardwick, P. Geology and regional setting of the Kuparuk oil field, Alaska. *American Association of Petroleum Geologists Bulletin* **67**, 1014-1031 (1983).

72. Bird, K. J. & Magoon, L. B. *Petroleum Geology of the Northern Part of the Arctic National Wildlife Refuge*. (US Dept Interior, USGS, *Geological Survey Bulletin* 1778, US Gov. Printing Office, 1987).

73. Bird, K. J. in *The Oil and Gas Resource Potential of the Arctic National Wildlife Refuge 1002 Area, Alaska, by ANWR Assessment Team* (US Dept Interior Rep., USGS Open-File Report, 1998).

74. Bird, K. J. in *Petroleum Resource Assessment of the National Petroleum Reserve in Alaska (*eds.Bird, K. J. & Nelson, P. E.) S1- GS4 (US Dept Interior, USGS, 2002).

75. Gryc, G. *Geology and Exploration of the National Petroleum Reserve in Alaska, 1974 to 1982* (US Dept Interior, USGS Professional Paper vol. 1399, 1988).

76. Mull, C. G., Houseknecht, D. W. & Bird, K. J. *Revised Cretaceous and Tertiary Stratigraphic Nomenclature in the Colville Basin, Northern Alaska* (US Dept Interior, USGS Professional Paper 1673, 2003).

77. Karlstrom, T. N. V. *et al. Surficial geology of Alaska,* scale 1:1,584,000 (US Dept Interior, USGS Misc. Geol. Inv. Map I-357, 1964).

78. Gesch, D. *et al*. The National Elevation Dataset. *Photogrammetric Engineering and Remote Sensing* **68**, 5-11 (2002).

79. For our analysis of seep spatial relation to geological faults, we compiled a fault GIS dataset for the state of Alaska using statewide data from (61,80) and more detailed local fault maps where available for southern Alaska[81], including high resolution neotectonic faults near Katalla (T. Pavlis, personal communication, May 14, 2010; and 49,82).

80. Plafker, G., Gilpin, L. M. & Lahr, J. C. Neotectonic map of Alaska, in *Geology of Alaska, Geology of North America, Decade of North American Geology* (eds. Plafker, G. & Berg, H. S.) v. G-1, plate 12, 1 map sheet, 1:2,500,000 scale; Digitized by S. Blatzi, Univ. of Wisconsin-Madison Space Science & Engineering Center (Geological Society of America, Boulder, 1994).

81. Miller, D. J. *Geologic map and sections of the central part of the Katalla District, Alaska* (US Dept Interior, USGS Miscellaneous Field Studies Map MF-722, 1975).

82. Wilson, F. H. *et al*. 2009. Digital files prepared by Wilson, F. H., Hults, C. P., Labay, K. A. & Shew, N. *Preliminary integrated geologic map databases for the United States: Preliminary geologic map of the Cook Inlet Region, Alaska including parts of the*

Talkeetna, Talkeetna Mountains, Tyonek, Anchorage, Lake Clark, Kenai, Seward, Iliamna, Seldovia, Mount Katmai, and Afognak, 1:250,000-scale (US Dept Interior Rep., USGS Open-File Report OFR 2009-1108, 2009).

83. R Development Core Team. *R: A language and environment for statistical computing.* (R Foundation for Statistical Computing, http://www.R-project.org, Vienna, 2009).
84. Conover, W. J., *Practical Nonparametric Statistics*, 3rd ed. (John Whitely & Sons., New York, 1999).
85. Etiope, G., Baciu, C., Caracausi, A., Italiano, F. & Cosma, C. Gas flux to the atmosphere from mud volcanoes in eastern Romania. *Terra Nova* **16**, 179–184 (2004).
86. Etiope, G., Feyzullaiev, A., Baciu, C. L., & Milkov, A. V. Methane emission from mud volcanoes in eastern Azerbaijan. *Geology* **32**, 465–468 (2004).
87. Johnsson, M. J. & Howell, D. G. *Thermal Evolution of Sedimentary Basins in Alaska* (US Dept Interior, USGS Bulletin 2142, 1996).
88. Dallimore, S. R. & Collett, T. S. *Scientific Results from the Mallik 2002 Gas Hydrate Production Research Well Program, Mackenzie Delta, Northwest Territories, Canada* (Geological Survey of Canada Bulletin 585, 2005).
89. Majorowicz, J.A. & Hannigan, P. K. Stability Zone of Natural Gas Hydrates in a Permafrost-Bearing Region of the Beaufort-Mackenzie Basin: Study of a Feasible Energy Source (Geological Survey of Canada Contribution No.1999275). *Natural Resources Research* **9**, 3-26, DOI: 10.1023/A:1010105628952 (2000).
90. Weitemeyer, K. A. & Buffett, B. A. Accumulation and release of methane from clathrates below the Laurentide and Cordilleran ice sheets. *Global and Planetary Change* **53**, 176-187 (2006).

91. Kroeger, K.F., di Primio, R., Horsfield, B., 2011. Atmospheric methane from organic carbon mobilization in sedimentary basins — The sleeping giant? ESR 107, 423-442.

92. Dimitrov, L.I. Mud volcanoes—A significant source of atmospheric methane. *Geo-Marine Letters* **23**, 155-161 (2003).

93. Leifer, I., Boles, J. R., Luyendyk, B.P. & Clark, J. F. Transient discharges from marine hydrocarbon seeps: spatial and temporal variability. *Environmental Geology* **46**, 1038-1052 (2004).

94. Leifer, I., Boles, J. R., Luyendyk, B.P. & Clark, J. F. Natural marine seepage blowout: Contribution to atmospheric methane. *Global Biogeochemical Cycles* **20**, GB3008, doi:10.1029/2005GB002668 (2006).

95. van Tatenhove, F. G. M., van der Meer, J. J. M. & Koster, E. A. Implications for deglaciation chronology from new AMS age determinations in central west Greenland. *Quat. Res*. **45**, 245-253 (1996).

96. Schiener, E. J. *West Greenland coal deposits: distribution and petrography* (Rapport Grønlands Geologiske Undersøgelse 77, 1976).

97. Petersen, H. I. Coal facies studies in Denmark and Greenland. *International Journal of Coal Geology* **58**, 53-59 (2004).

98. Gregersen, U. & Skaarup, N. A mid-Cretaceous prograding sedimentary complex in the Sisimiut Basin, offshore West Greenland—stratigraphy and hydrocarbon potential. *Marine and Petroleum Geology* **24**, 15-28 (2007).

99. Hoekstra, P. Moisture movement in soils under temperature gradients with the cold-side temperature below freezing. *Water Resour. Res.* **2**, 241–250, doi:10.1029/WR002i002p00241 (1966).

100. McCauley, C. A., White, D. M., Lilly, M. R., & Nyman, D. M. A comparison of hydraulic conductivities, permeabilities and infiltration rates in frozen and unfrozen soils. *Cold Regions Science and Technology* **34**, 117-225 (2002).

101. Kleinberg, R. L. & Griffin, D. D. NMR measurements of permafrost: unfrozen water assay, pore-scale distribution of ice, and hydraulic permeability of sediments. *Cold Regions Science and Technology* **42**, 63-77 (2005).

102. Taylor, A. E., Dallimore, S. R. & Wright, J. F. in *Proceedings of the Ninth International Conference on Permafrost* (eds. Kane, D. L. & Hinkel, K. M.) 1757-1762 (Institute of Northern Engineering, Fairbanks, 2008).

103. Tarnocai, C. *et al*. Soil organic carbon pools in the northern circumpolar permafrost region. *Global Biogeochem. Cycles* **23**, GB2023 (2009).

104. Boswell, R. & Collett, T. S. Current perspectives on gas hydrates resources. *Energy Env. Sci*. doi: 10.1039/C0EE00203H (2011).

105. Gregersen, S. Intraplate earthquakes in Scandinavia and Greenland neotectonics or postglacial uplift. *J. Ind. Geophys. Union* **10**, 25-30 (2006).

106. Ekström, G., Nettles, M. & Abers, G.A. Glacial earthquakes. *Science* **302**, 622-624 (2003).

107. Arctic regions underlain by thick, old continuous permafrost[70,108,109] have been 'capping' gas percolating from deeper, leaky hydrocarbon reservoirs since the early Pleistocene[15,70,89]. In contrast, discontinuous permafrost that forms during glacial periods and disappears partially under milder interglacial climate regimes on time scales of 10^2-10^4 years[110-112], should trap less gas from below, and consequently release less gas during its phases of thaw. Similar conclusions were drawn in studies modeling the response of

onshore gas accumulations and release associated with permafrost and ice sheet fluctuations during glacial-interglacial cycles on a northern Germany petroleum system[14], the United States Antrim Shale Formation[13], and CH_4 hydrates beneath the Laurentide and Cordilleran ice sheets[90].

108. Andreev, A. A. *et al*. Late Saalian and Eemian palaeoenvironmental history of the Bol'shoy Lyakhovsky Island (Laptev Sea region, Arctic Siberia). *Boreas* **33**, 319-348 (2004).

109. French, H. M. *The Periglacial Environment*, 3rd ed. (John Wiley and Sons, England, 2007).

110. Péwé, T. L. *Quaternary geology of Alaska*. (US Dept Interior, USGS Professional Paper 835, 1975).

111. Froese, D. G., Westgate, J. A., Reyes, A. V., Enkin, R. J. & Preece, S. J. Ancient permafrost and a future, warmer Arctic. *Science* **321**, 1648 (2008).

112. Reyes, A. V., Froese, D. G., Jensen, B. J. L. Permafrost response to last interglacial warming: field evidence from non-glaciated Yukon and Alaska. *Quat. Sci. Reviews* **29**, 3256-3274 (2010).

113. Kaufman, D. S. & Manley, W. F. in *Quaternary Glaciations - Extent and Chronology, Part II, North America: Developments in Quaternary Science* vol. 2b (eds. Ehlers, J. & Gibbard, P. L.) 9-27 (Elsevier, Amsterdam, 2004).

114. Chapman, R. M., Detterman, R. L. & Mangus, M. D. *Geology of the Killik–Etivluk Rivers region, Alaska*. (US Dept Interior, USGS Professional Paper 303-F, 1964).

115. Itta, F. Personal communication of her observation of gas seepage from the Qalluuraq Lake near Atqasuk since 1945 (2011).

116. Euskirchen, S. E. *et al*. Importance of recent shifts in soil thermal dynamics on growing season length, productivity, and carbon sequestration in terrestrial high-latitude ecosystems. *Global Change Biology* **12**, 731-750 (2006).

117. Ruppel, C. D. Methane hydrates and contemporary climate change. *Nature Education Knowledge* **2**, 12 (2011).

118. Hampel, A., Hetzel, R. & Maniatis, G. Response of faults to climate-driven changes in ice and water volumes on Earth's surface. *Phil. Trans. R. Soc. A.* **368**, 2501-2517 (2010).

119. Chalmers, J. A., Pulvertaft, T. C. R., Marcussen, C. & Pedersen, A. K. New insight into the structure of the Nuussuaq Basin, central West Greenland. *Marine and Petroleum Geology* **16**, 197-224 (1999).

120. Holdgate, G. R. *et al*. Inorganic chemistry, petrography and palaeobotany of Permian coals in the Prince Charles Mountains, East Antarctica. *International Journal of Coal Geology* **63**, 156-177 (2005).

121. Macdonald, D. I. M. *et al*. A preliminary assessment of the hydrocarbon potential of the Larsen Basin, Antarctica. *Marine and Petroleum Geology* **5**, 34-53 (1988).

122. Westermeyer, W. Resource allocation in Antarctica: A review. *Marine Policy* **6**, 303-325 (1982).